IJREAT International Journal of Research in Engineering & Advanced Technology, Volume 2, Issue 6, Dec-Jan, 2015
ISSN: 2320 – 8791 (Impact Factor: 1.479)
www.ijreat.org

Design And Simulation Of Multi Cell Interleaved Fly Back Converter

P.Harika[1], K.Pavankumar Goud[2], Damodhar Reddy[3]

[1,2,3]Ass.Prof, VCC & JPNCE, Telangana

ABSTRACT:

The aim of this project is to design and implement a converter with a high power density. The main function is to feed a 20kW/400V load from the 22V DC of an embedded network with galvanic insulation. A low-input voltage high-power topologies are implemented using an Intercell transformer constituting interleave converter stages with desired specifications. These specifications require a galvanic insulation and the topology is the Intercell Transformer (ICT) fly back converter. In the first section the operating principle of the ICT fly back converter is discussed. Here the ICTs are implemented as monolithic devices or can also be implemented as separate ICT devices and the storage inductance required for the fly back operation is the leakage inductance between the two primary windings.

The second part presents the main features of the Intercell transformer design which includes the choice of the cell number. The last part is about the design and the implementation of the complete fly back converter using ten cells. The evolution of the current ripple versus duty cycle relates to a ten-
cell design which demonstrates the topology that needs only one level of magnetic components.

Interleaving the control signal of the switches produces the waveforms and the interval allows in choosing the coupling between phases and thus the ICT common-mode inductance (the storage inductance). The AC ampere turns can be split in two components as differential mode and common-mode components. The two halves of secondary windings are made using a PCB technology.

The aim is to minimize the turn-off losses and also to recover the energy stored in the leakage inductance of winding secondary windings have been made using a multilayer PCB with a Kapton base. The mechanical and thermal assembly has been designed to maximize the power density by optimizing the positioning of discrete and standard devices. Different digital solutions can be used to realize a multicell control. A preliminary work concerns the choice, design and the test of each cell elements, mainly the transformer and the primary switching stage. The experimental results are presented and discussed here using MATLAB / Simulink. Interleaved multi cell converters are now widely used for low-voltage/high-current applications.

INTRODUCTION

1.1 Introduction

INTERLEAVED multicell converters are now widely used, especially for low-voltage/high-current applications. Among which voltage regulator module (VRM) is probably the most prominent example. Other emerging application fields of these topologies are provided by systems connected to low-voltage energy sources and storage elements as photovoltaic (PV) arrays, fuel cells, batteries, ultra capacitors, especially when these systems are onboard and weight and space savings are required.

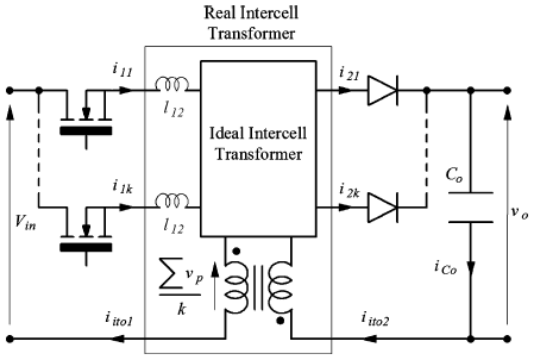

Fig. 1.1 General topology of the ICT flyback converter.

The aim of this project is to present the design and implementation of a converter with a high power density; the main function is to feed a 20 kW/400 V load from the $22V_{dc}$ of an embedded network with galvanic insulation. The specifications of this converter for the considered application are as follows.

1) Input voltage: 22V DC.
2) Output voltage 400V DC.
3) Output power: 20kW.
4) Weight: to be minimized.

These specifications lead the authors to design an original converter, the ICT-based multi cell fly back. This topology recently described, seems in adequation with such specifications, but its relatively complex operation requires developing a specific know-how; the authors have thus tried to push the design one step further to evaluate more precisely the potential of this topology.

In the first section, the basic properties of ICT-based multi cell flyback are recalled. Other points of interest such as the design of the ICTs and the number of cells are then discussed in a second section. Last, the different steps of the design and the experimental results are described.

1.2 Objective of the Thesis

The objective of the project is to design and implement a converter with a high power density. The main function is to feed a 20 KW/400V load from the 22 V DC of an embedded network with galvanic insulation. A low-input voltage high-power topologies are implemented using an Intercell transformer constituting interleave converter stages with desired specifications. These specifications require a galvanic insulation and the topology is the Intercell Transformer (ICT) fly back converter.

1.3 Organization of the Thesis

In this present work, MATLAB/SIMULINK model of the Interleaved multi cell fly back converter interleaved converters are now widely used for low-voltage/high-current is developed. The thesis is organized in six chapters.

- In the first Chapter introduce to the basic introduction of about the interleaved multi cell fly back converter, Problem Formulation & Literature survey are presented.
- The Chapter two introduces to DC to DC converter of Buck Converter Step-Down Converter, Boost Converter Step-Up Converter and Buck-Boost Converter.
- The Chapter three discusses Structure and principle Flyback Converter On and Off state and also explains Operation of the flyback converter.
- The construction of Intercell transformer is explained in the Chapter four.
- Chapter five is modeling of case study by Intercell Transformer flyback converter topology
- Design and Results of Simulation diagram are discussed In the Chapter six.

2. MODELING OF INTERCELL TRANSFORMER FLYBACK CONVERTER

2.1 Intercell Transformer flyback converter topology

The proposed solution is appropriate for low-voltage/high power applications. In this field, bridge or half-bridge topologies are penalized by the conduction losses into the power switches. In this context, the parallel assembling of power switches is necessary in the case of a single converter and an interesting option, frequently used by the designers, is to parallelize the converters rather than switches.

The global converter is more complex but all components, switches, magnetic devices, capacitors, are easier to design and to build. In addition, the interleaving operating mode allows reducing drastically the input and output filters. So, the Intercell transformer flyback is a good option although it is obviously not the only one.

The more efficient classical topology in this context is the push-pull Fig. 2.1a. The proposed flyback, in a more realistic version with single-switch cells Fig. 2.1b, needs to be further evaluated in comparison with this reference. By supposing the same interleaving level k in the two cases, for the same total power P, k/2cells are necessary for the push pull and k for the flyback, k having to be even for the push-pull. So, the modular characteristic of the flyback is better.

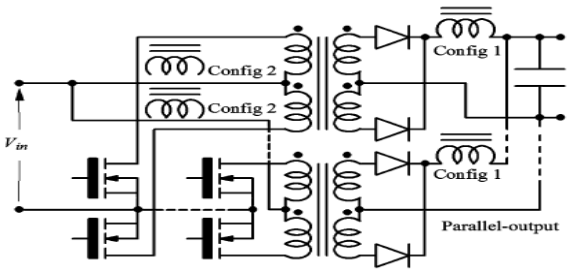

Fig.2.1(a). Push-pull

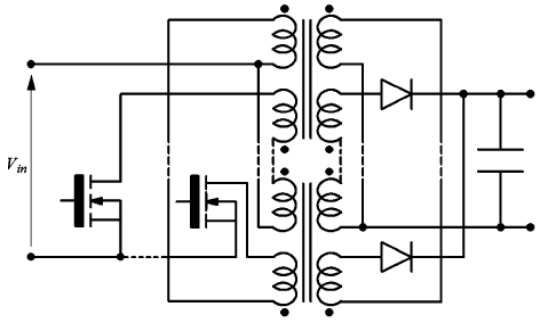

Fig.2.1(b). Intercell transformer flyback

Fig. 2. Topologies of push-pull and flyback for comparison

Then, the push-pull requires k switches, k diodes, k/2 transformers, and k/2 output or input inductors, while the flyback requires the same number of switches and diodes but k transformers and no inductor. The different electrical stresses are similar in the two cases. So the main difference results of the higher dividing up of the transformers in the flyback.

This can be considered an advantage (transformer easier to built, increase of the total thermal exchange surface), as well as a drawback (twice more transformers, interconnections), that can be balanced by the suppression of inductors. In the two topologies, the power reversibility can be provided by adding anti parallel switches on the secondary side and anti parallel diodes on the primary side. In fact, this fast comparison shows many similarities between the two topologies. Nevertheless, in the author point of view, several features could make the Intercell transformer flyback attractive.

- It is very modular a1nd well-suited to the design of converter ranges, with the possibility to realize high-power converters by using standard medium size cores for the transformers
- The suppression of inductors is a significant advantage, particularly for the low-voltage/high-current applications.
- Compared to the interleaved topologies using separated inductors, the characteristic impedance of the output filter is significantly lower with the Intercell transformer topologies, property very interesting in case of applications requiring high dynamic performances of the output regulation

The ICT fly back converter has been detailed. Fig.2.2. displays the topology of such an ICT flyback converter with *k* cells.

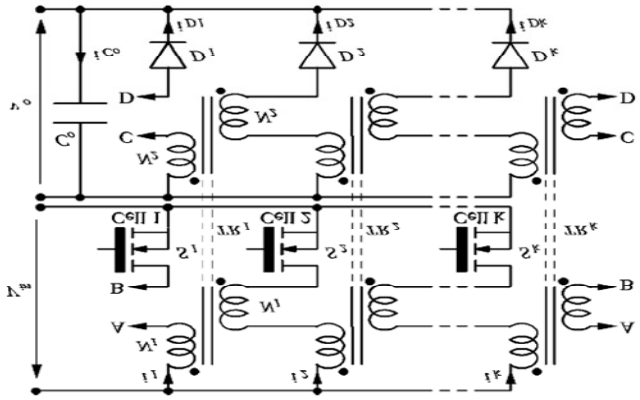

Fig. 2.2. ICT flyback converter with separated transformers
(*T* switching period, $i_{ito} = i_{ito1} + n_2 / n_1 \, i_{ito2}$).

It has been shown that ICTs can be implemented either as monolithic devices or as separate devices. The second form is used in this paper, according to the circuit shown in Fig. 2.2. Each elementary transformer comprises four windings (two primaries and two secondaries), so that *k* such devices can be arranged to form a *k*-phase ICT. In this configuration, the storage inductance L_{ito1} (respectively, L_{ito2}) required for the flyback operation is the leakage inductance between the two primary windings (respectively, secondary).

To clarify next sections, this leakage inductance will be named in the following ICT common-mode inductance. The leakage inductances shown in Fig. 2.2, (l_{12}) are related to the coupling coefficient between homologous primary and secondary windings.

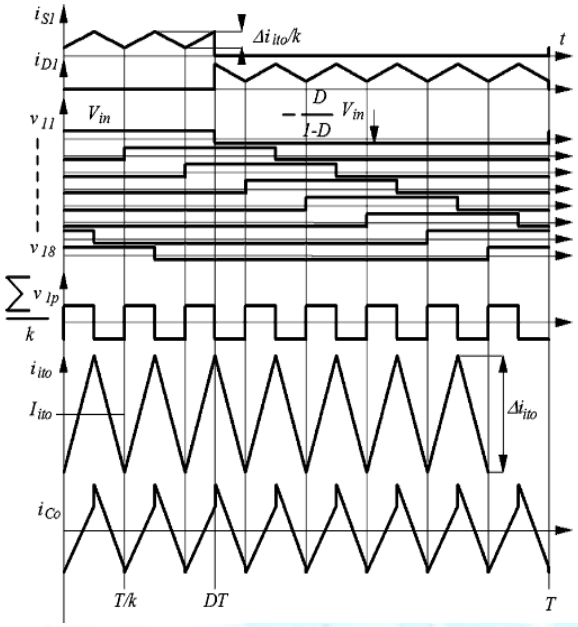

Fig. 2.3. Theoretical waveforms of the ICT fly back converter (*F* switching frequency).

Interleaving the control signal of the switches produces the waveforms shown in Fig. 2.3. These waveforms are given for the eight-cell configuration, which is chosen in the last section of this paper. Due to interleaving and relatively high number of cells, a low value of the storage inductance can be used. Building the transformer so as to obtain an ICT common-mode inductance that is only slightly above the minimum feasible leakage inductance, the continuous conduction mode of the flyback is obtained.

An optimal fly back ICT with a very low dc flux and no air gap is thus obtained. Its design is almost only related to the ac components, and is therefore, similar to a transformer design.

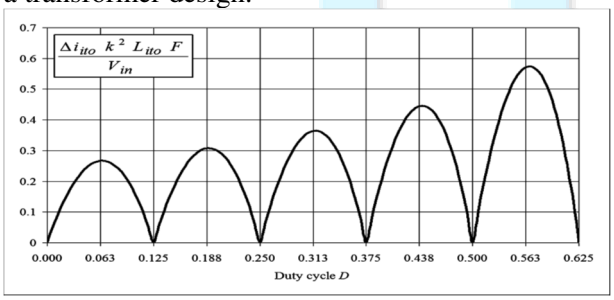

Fig. 2.4 Current ripple in ICT fly back converter (example of eight cells)

The evolution of the current ripple versus the duty cycle is given in Fig. 2.4, which still relates to an eight-cell design. Like other interleaved converters, the current ripple is minimized for duty cycles multiple of $1/k$, but unlike interleaved buck converters, the local maxima are different

$$\Delta i_{ito} = \frac{[kD-q+1][q-kD]}{1-D}\ \frac{V_{in}}{k^2 L_{itoF}} \quad \ldots\ldots\ldots\ldots\ldots\ldots (2.1)$$

2.2 General Features of the Design

2.2.1 ICT

The design of ICT is somewhat specific especially because of the shape and the distribution of the currents among the different windings. This is summarized in Fig. 2.5 related to transformer TR2.

Since planar transformers are to be used, the four windings should be stacked vertically with an interval of height *ha* separating the windings of one phase from the windings of the other phase. The interval allows choosing the coupling between phases and thus the ICT common- ode inductance (the storage inductance).

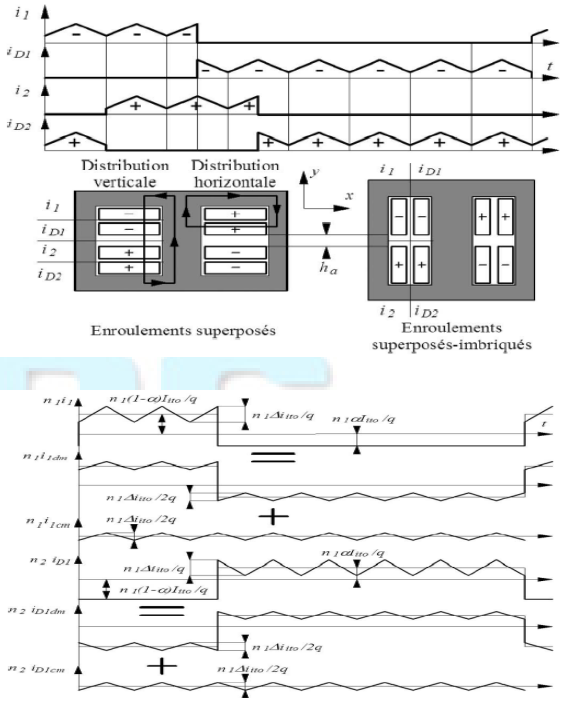

Fig. 2.5 Current distributions in the windings of ICT

For one phase, the ac ampere turns can be split in two components: the differential-mode and common-mode components. As can be seen from the waveforms

in Fig. 5.5, the differential mode components of currents i_k and i_{Dk} are in opposition like in a standard transformer. A 1-D model including eddy-current effects can thus be applied to calculate the copper losses in each of the two groups i_1 , i_{D1} and i_2 , i_{D2} . The losses in the two groups are identical. The common-mode components have the same amplitudes in all four windings but they have different signs. The 1-D approach still applies if an equivalent primary composed the two windings of phase 1 and an equivalent secondary composed the two windings of phase 2 are considered. The total joule losses are then the sum of the losses generated by the two components (differential mode and common mode), and are thus, easily calculated.

A complete design method of the ICT has been presented. It involves deriving from the specifications (power, ambient temperature, frequency, current ripple, winding geometry, etc.), the core and copper losses, the heat exchange area, the operating temperature and, in the end, the number of turns and all the dimensions of the ICT.

2.2.2 Number of Cells

The choice of the number of cells is another crucial point of the design. Using the method described, several designs have been made for different number of cells and switching frequencies. This preliminary study has been made with the specifications of the application described in the last section of the present paper, namely V_{in} = 22 V, V_{out} = 600 V and a power of 12 kW. Planar cores are a priori chosen, because they are compatible with the high power density specification.

On the other hand, it is difficult to obtain high values of leakage inductance with these cores, and a relatively high current ripple is used in the chosen design. A standard ferrite material has been selected in accordance with the frequency. The key characteristics of these designs are represented in Fig. 2.6. The first set of curves gives the total volume of the k transformers, each of them comprising a planar $E + I$ core and four windings. The characteristic dimension is the width of the core, which is generally used as a reference by ferrite manufacturers. The discretization of existing cores is not accounted for in the design routine (in this case relevant standard dimensions are 64, 58, and 43 mm).

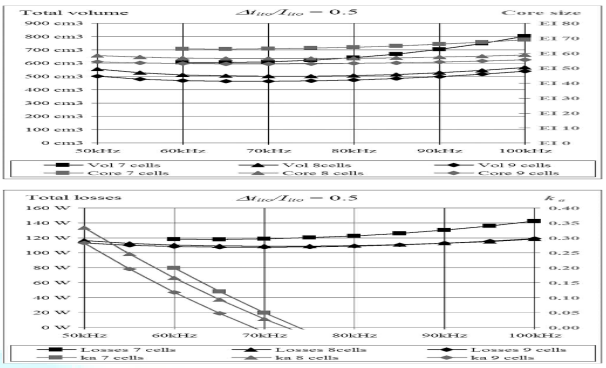

Fig. 2.6. Influence of the cell number

These first curves show that with eight cells or more, the total volume is acceptable and that it is possible to use standard core EI 58. Using nine cells still does not allow using standard cores one size smaller (43 mm).

The second set of curves gives the estimated total losses in the k cells as well as the value of $ka = ha/lw$ (see Fig. 5.7.) giving a current ripple of 50%. Once again, no significant gain is obtained when increasing the cell number to more than eight. It should also be noted that reasonable ka values are rapidly obtained. Above 70kHz, the intrinsic leakages are enough for storage, which reveals a great similarity with the design of a standard transformer.

Based on these results, eight cells are used in the implementation described in the next section. The choice of an even number of cells allows a symmetrical layout, which is generally an advantage. The switching frequency is kept relatively low (50 –60kHz), which gives similar results and reduces the design problems associated with the switching stages.

2.3 Design of the 22 V-To-400 V/20 KW ICT Flyback converter

Designing an ICT fly back converter for these specifications has been decided with two aims in view: demonstration of the feasibility of this topology, and evaluation of its performance in this low-voltage high-power context for which paralleling converters or cells is quasi-compulsory. Because of the relative complexity of the complete converter, a first step was to design and test the elements of a single cell, namely, an elementary transformer and a commutation cell of 1500W (12 KW/8).

2.3.1. Intercell Transformer

The design of the elementary ICT has been initiated using the general results presented in Section III-B. Then, additional implementation constraints of the windings have been taken into account. The elements of this design are summarized in Table I. The two primary windings are made of a single and massive layer of copper with a thickness of 0.8mm. As shown in Fig. 2.7, these windings are sandwiched between two halves of secondary windings with six turns each.

TABLE I
2.1 ICT Design

E + I 58 planar, ferrite N87, $\Delta T = 60^o$ C			
P = 1.5kW	F = 51kHz	$\Delta B_M = 0.22T$	$J_{RMS} = 5A/mm^2$
$P_{core} = 4.5W$	$P_{wind} = 9.5W$	$K_a = 0.26$	$\Delta i_{ito}/ I_{ito} = 0.53$
Primary layer (2 x 1 turn) 19mm x 0.8mm		Secondary layers (4 x 6 turns) 19mm x 0.07mm	

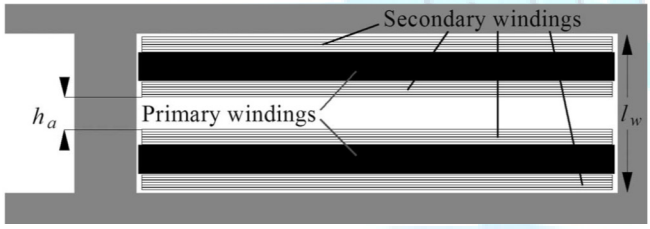

Fig.2.7. Winding arrangement

The two halves of secondary windings are made using a PCB technology. For the first prototype, double-sided epoxy PCB isolated with a Kapton foil was assembled to form the complete winding [see Fig. 2.8(a)]. For the final device, the two halves of secondary windings have been made using a multilayer PCB with a Kapton base [see Fig. 2.8(b)]. An experimental setup described made it possible to generate currents with the same characteristics as those of the actual converter and to test the prototype cell. The results obtained confirmed the design and the technology to be used.

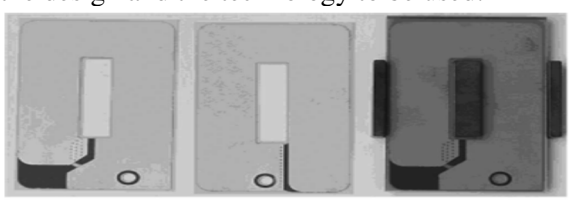

Fig. 2.8. Secondary windings (a) Secondary windings of the test ICT.

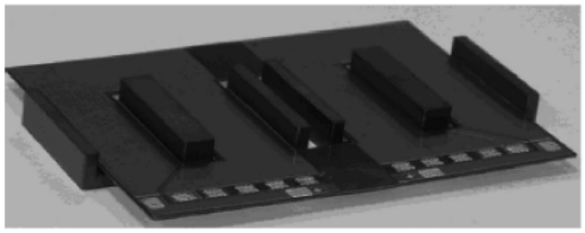

(b) Final secondary windings

2.3.2 Primary Switching Stages

The implementation of low voltage high current is never easy. In this case, 150A needs to be switched under a theoretical voltage of 60V. Like for the ICT, a switching stage has been designed, implemented, and tested in order to check the final design of the elementary commutation cell.

The aim is not only to minimize the turn-off losses, but also to recover the energy stored in the leakage inductance of the ICT and in the connexions stray inductance. The equivalent inductance is estimated to be 100nH per cell, which would amount to 60W of losses per cell if not recovered. Two options have been considered, the active clamp [see Fig. 2.9(a)] and the nondissipative snubber [see Fig. 2.9(b)].

These solutions have been evaluated in a buck–boost configuration that recreates the conditions of the fly back while making the preliminary test described further on easier. Various simulations and tests have been made to compare these two options. The first one turns out to be pretty bad fit for low voltage and this switching frequency. The values of the reactive components are quite high; several tens of microfarads for the clamp capacitor when a 1-μH inductor is used, which is a bulky capacitor if we consider the high-rms current. In addition, the clamp switch also flows a very high current.

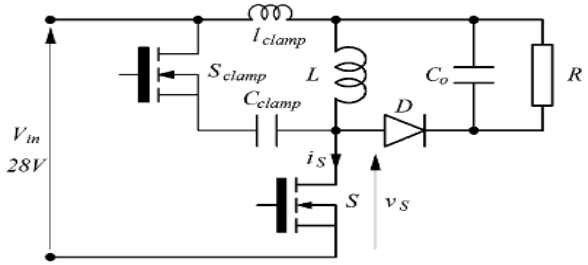

Fig.2.9. Switching stages (a) Active clamp.

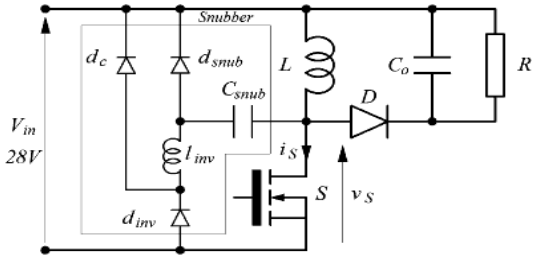

(b) Nondissipative snubber

The main advantage of the nondissipative snubber is that the values of the different components are not related to the switching frequency. A simple 2 μF allows recovering the leakage energy and the inverting inductor (2 μH) flows a current that is way smaller than the switch current.

This solution was finally chosen for the complete system. It should be noted that the active clamp becomes attractive again if the switching frequency and the input voltage are increased.

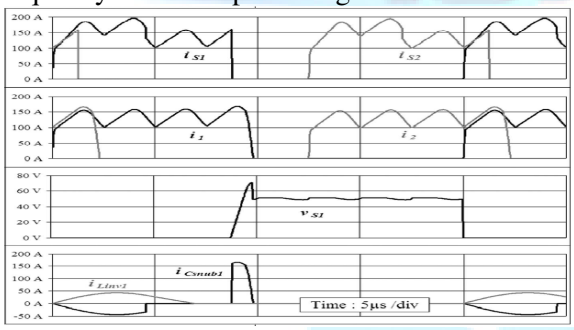

Fig.2.10. Simulation of the ten-cell converter with nondissipative snubbers.

This solution has been tested by simulation in a complete eight-cell converter to measure the influence of the coupling. A result is shown in Fig. 2.10. Although the snubber slightly modifies the waveforms, we came to the conclusion that it is compatible with the multicell topology.

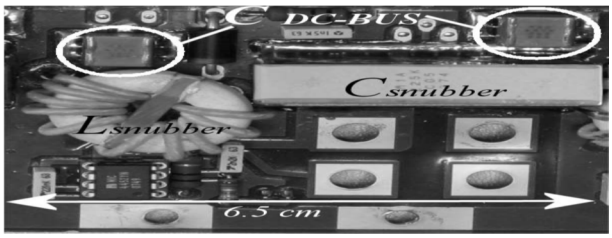

Fig. 2.11. Top-view of the final switching cell implantation

The circuit shown in Fig. 2.9(b) has been implemented using the power MOSFET selected for the final converter (IXUN350N10, ISOTOP package, *V*DSS = 100 V, *I*dc (25◦C) = 350 A, *R*DSON (25◦C) = 1.9 mΩ). Fig. 2.11, shows the final implantation of a switching cell that gives an idea of the snubber component sizes. Each cell also includes two dc-bus capacitors (2 × 6.8 μF). Consequently, the total value of the distributed dc-bus capacitor is 109 μF.

This setup was successfully tested using a very compact layout and using ceramic capacitors. An experimental result is shown in Fig. 5.13.

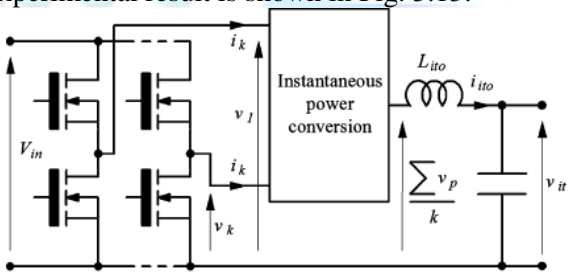

Fig. 2.12. Interleaved converters using IT (a) Interleaved buck.

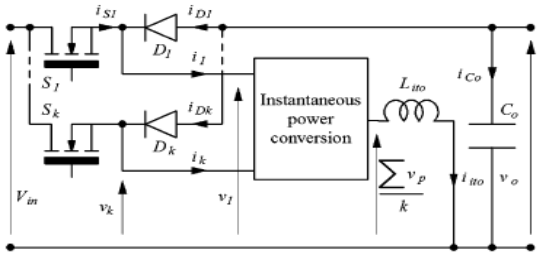

(b) Interleaved buck-boost

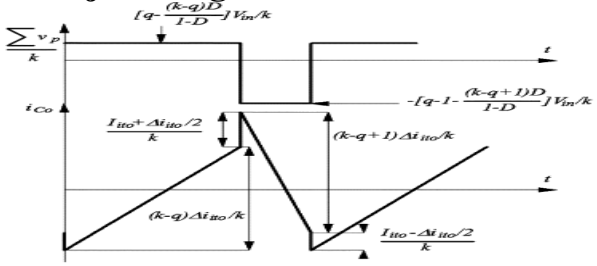

Fig. 2.13. Nondissipative snubber—experimental results on a buck–boost

2.3.3 Secondary Rectifier

The first design planed the use of one 1200 V– 10 A PIN diode per cell. In fact, this solution leads to unacceptable recovery losses. The current solution uses two series-connected 600 V– 12 A diodes associated with parallel *R–C* balancing circuits. PIN diodes and SiC diodes will be tested. Despite the addition of two voltage drops, this second configuration is more efficient due to the drastic reduction of recovery losses (see Table II and Section IV-F).

2.3.4 Mechanical and Thermal Assembly

The mechanical and thermal assembly has been designed in the aim to maximize the power density, mainly by optimizing the positioning of discrete and standard devices. The eight-cell converter has been built using a liquid-cooled cold plate with a 1 kW handling capability.

All semiconductors and ICTs are mounted on this plate. All electrical connections are made using a PCB except for the primary windings and the 28V bus bar.

Fig. 2.14, shows a preliminary 3-D CAD view and a picture of the actual converter. The overall size is 23 cm × 20 cm × 5 cm, which gives a specific power of 4.5 kW/*l*.

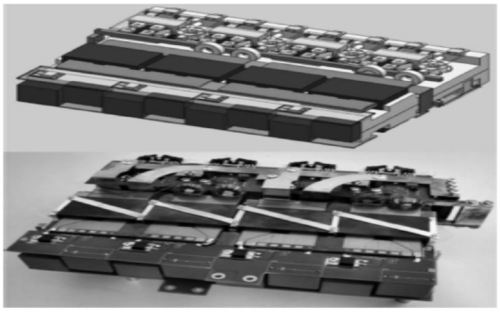

Fig. 2.14. 3-D design view and real converter

2.3.5 Control Stage

Different digital solutions can be used to realize a multicell control stage. The present one is made using a field-programmable gate array (FPGA) that precisely tunes the duty cycles of the different cells. This is required to balance the currents in the different cells in open loop and allows the validation that is made here.

A closed-loop configuration is currently in progress using the same control system. Different techniques exist to realize the current balancing of multiparallel interleaved converters. For example, VRMs using ICTs, with high number of cells and current-controlled are now mounted on motherboards to supply the CPU. Therefore, the feasibility of such topologies operating in closed loop has been demonstrated. The aim of the development concerning the ICT fly back converter is to implement the simplest closed-loop solution, especially in regard with the number of sensors.

2.3.6 Power Losses Estimation

Estimated losses, deduced from datasheets (semiconductor devices) or from measurements (ICTs) are given in Table II. Two configurations are compared, the first using one high-voltage rectifier diode per cell, and the second using two medium voltage series-connected diodes (cf., Section IV-C). This global estimation emphasizes the heavy part of primary losses, consequence of the high current level at the low-voltage side. For example, the snubber losses (diodes and inductor) are significant and cannot be neglected. This drawback should be the same with any switching-aid network.

Additional losses have been approximately estimated to take into account the connections and the effect of stray capacitances resulting in the high transfer ratio of the ICTs.

TABLE II

2.2 Losses Estimation

	Secondary configuration	
Estimated losses parts	Rectifier Diodes 1 x 1200V – 10A	Rectifier Diodes 2 x 600V – 10A
On – losses in	300W	300W

MOSFETs		
Snubberr losses	200W	200W
ICT losses (Winding, Core)	120W (80W, 40W)	120W
On – losses in diodes	80W	140W
Recovery losses in diodes	320W	30W
Additional losses*	100 to 200W	100 to 200W
Total	1110 to 1210W	880 to 980W
Efficiency	91.5 to 90.85 %	93 to 92.5%

*primary connections, stay capacitances

3. SIMULATION DESIGN AND RESULTS

3.1. Simulation Design

The flyback converter is developed as an extension of the Buck-Boost converter. The basic flyback converter consists of an inductor and is replaced by a transformer. The buck-boost converter works by storing energy in the inductor during the ON phase and releasing it to the output during the OFF phase. With the transformer the energy storage is in the magnetization of the transformer core.

To increase the stored energy a gapped core is used. The Low – Voltage (22V) high-power concept is paralleling converters or cells using Intercell Transformer constituting of converter stages. This structure converts the Low Voltage to High Power DC/DC, an attractive solution for meeting specifications required. The ICT flyback converter needs only one magnetic component per cell, and avoids the drawbacks of the single-cell flyback converter as show in Fig. 3.1. The resultant wave forms of the buck boost converter voltage and current waveforms as shown in Fig. 3.2 , Fig. 3.3 and Fig. 3.4.

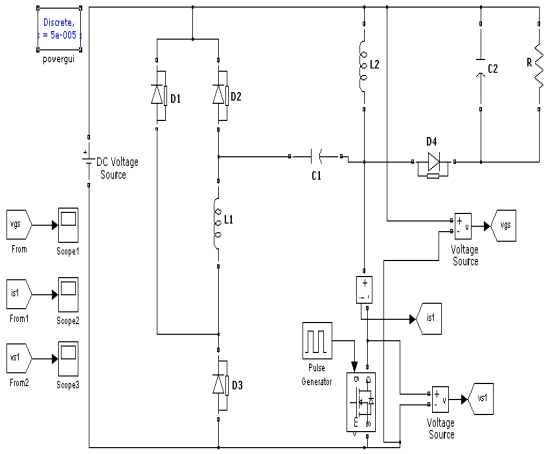

Fig. 3.1. Simulation of the buck–boost

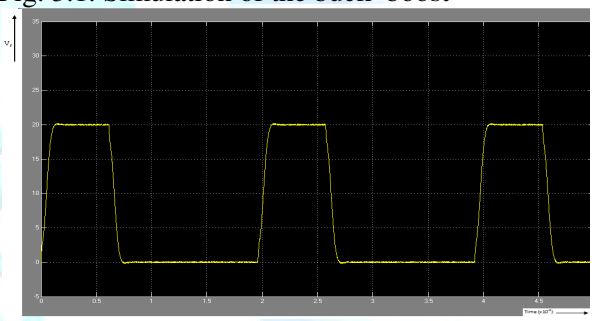

Fig.3.2. Input Voltage of Buck- Boost Converter

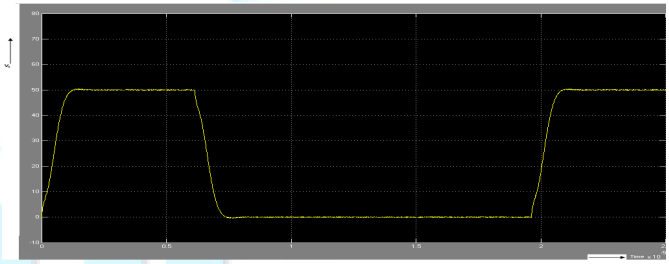

Fig. 3.3. Output Voltage of Buck Boost Converter

The converter of buck- boost flyback converter current in dc simulation of as shown in Fig. 2.4.

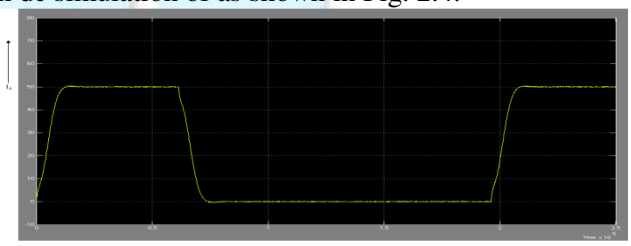

Fig. 3.4. Buck- Boost Flyback converter Current

3.2 Simulation of Multi Cell Interleaved Fly Back Converter

The main function is to feed a 20kW/400V load from the 22V DC of an embedded network with galvanic insulation. A low-input voltage high-power topologies are implemented using an Intercell transformer constituting interleave converter stages with desired specifications. These specifications require a galvanic insulation and the topology is the Intercell Transformer (ICT) fly back converter.

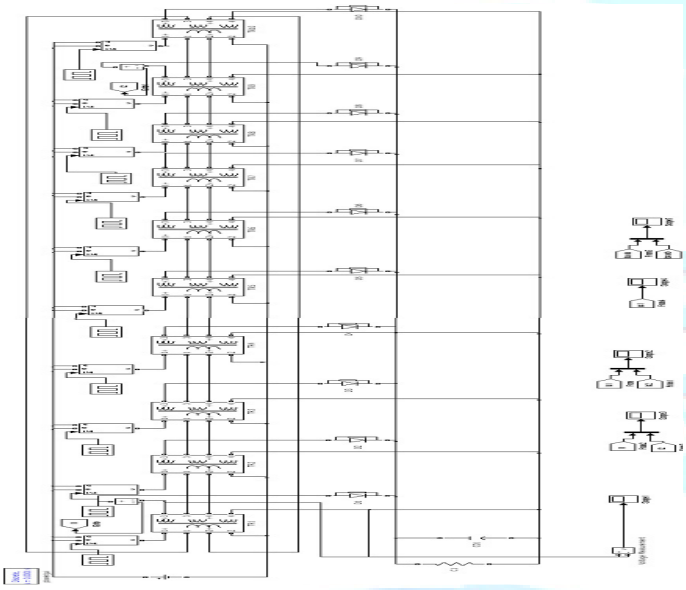

Fig 3.5, 10-Cell Interleaved Transformer fly back Converter

The results obtained for the 20kW rated power are shown Fig. 3.6. The waveforms are quite different from the simulated ones, due to the effect of higher stray capacitances of the windings (approximately 50nF per cell, seen from the primary side) that are resonating with the stray inductances.

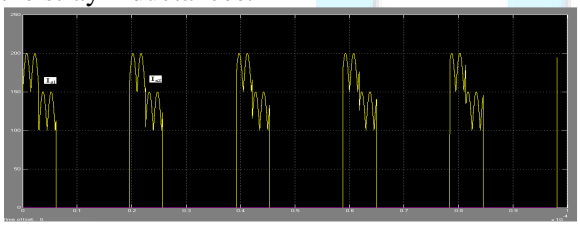

Fig. 3.6. Experimental input waveforms—22V–50kHz–20kW

The waveforms shown in Fig. 3.7 have been obtained with reduced switching frequency (25kHz) and voltage (22V), leading to an output power limited to 20kW, for the output nominal current. This configuration has been chosen for better exhibition of the classical shapes of currents in the ICT topology. In this case, the influence of stray capacitance is lower; therefore, the results are quite similar to those given by the simulations, and clearly show the theoretical k F current ripple.

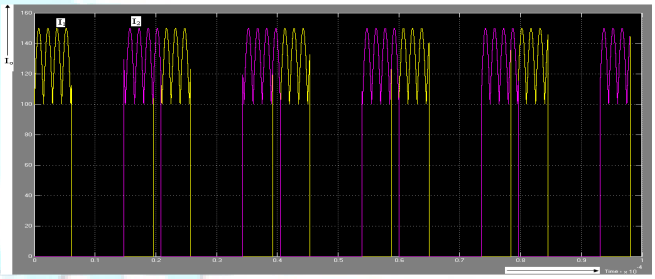

Fig. 3.7. Experimental output waveforms

This solution has been tested by simulation in a complete ten-cell converter to measure the influence of the coupling. A result is shown in Fig. 3.8 and Fig. 3.9. Although the snubber slightly modifies the waveforms, we came to the conclusion that it is compatible with the multicell topology.

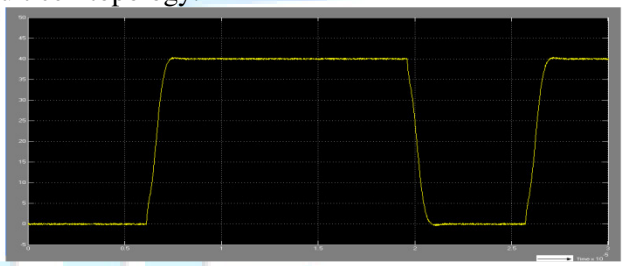

Fig 3.8. Simulation of the Ten-cell converter with nondissipative snubbers

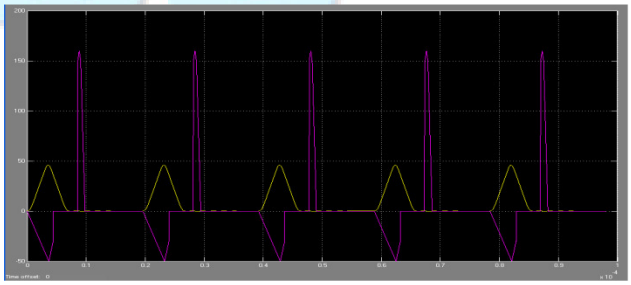

Fig 3.9. Nondissipative snubbers—experimental results on Ten-cell converter

CONCLUSION

The topology and the operating mode of the Intercell Transformer (ICT) fly back converter have been first recalled. This structure is an attractive solution for answering to specifications requiring the interleaving of insulated power stages. The ICT fly back converter needs only one magnetic component per cell, and avoids the drawbacks of the single-cell fly back converter. To confirm its interest, the design and the realization of a 22V–20kW demonstrator is proposed. The design and the experimental tests of one cell are first made. Then, an advanced packaging of the complete ten-cell converter is defined and realized. The experimental results show the need of some technological improvements, but above all show the real viability of the proposed topology. The modular form of the single magnetic stage is one of the most attractive properties of the topology, making of this solution a good candidate to reach high values of power density.

REFERENCES

[1] Franc¸ois Forest, Bertrand G´elis, Jean-Jacques Huselstein, Bernardo Cougo, Eric Labour´e, "Design of a 28 V-to-300 V/12 kW Multicell Interleaved Flyback Converter Using Intercell Transformers" *IEEE Trans. on Power Electronics*, vol. 25, no. 8, pp. 1966-1974, August 2010.

[2] F. Z. Peng, H. Li, G.-J. Su, and J. S. Lawler, "A new ZVS bidirectional DC–DC converter for fuel cell and battery application," *IEEE Trans. Power Electron.,* vol. 19, no. 1, pp. 54–65, Jan. 2004.

[3] Huafeng Xiao, Liang Guo and Shaojun Xie, "A ZVS bidirectional DC–DC converter with phase shift plus PWM control scheme," *IEEE Trans. Power Electron.*, vol. 23, no. 2, pp. 943–948, Mar. 2008.

[4] Quan Li and Peter Wolfs, " A Current Fed Two-Inductor Boost Converter With an Integrated Magnetic Structure and Passive Lossless Snubbers for Photovoltaic Module Integrated Converter Applications," in *IEEE Trans. On Power Electronics,* VOL. 22, NO. 1, January 2007.

[5] J. Li, C. R. Sullivan, and A. Schultz, "Coupled inductors design optimization for fast-response low-voltage DC-DC converters," in *Proc. APEC 2002*, vol. 2.

[6] F. Blaabjerg, Z. Chen, and S. B. Kjaer, "Power electronics as efficient interface in dispersed power generation systems," *IEEE Trans. Power Electron.*, vol. 19, no. 5, pp. 1184–1194, Sep. 2004.

[7] F. Forest, T. Meynard, E. Labour´e, V. Costan, and J.-J. Huselstein, "A multi-cell interleaved flyback using intercell transformers," *IEEE Trans. Power Electron.*, vol. 22, no. 5, pp. 1662–1671, Sep. 2007.

[8] Franc¸ois Forest, Eric Labour´e, Bertrand G´elis, Vanessa Smet, Thierry A. Meynard and Jean-Jacques Huselstein, "Design of Intercell Transformers for High-Power Multicell Interleaved Flyback Converter," *IEEE Trans.s on Power Electronics*, VOL. 24, NO. 3, pp. 580- 590, March 2009.

[9] Eric Labouré, Alain Cunière, T. A. Meynard, Francois Forest and Emmanuel Sarraute, "A Theoretical Approach to InterCell Transformers, Application to Interleaved Converters," *IEEE Trans. on Power Electronics*, VOL. 23, NO. 1, pp. 464- 472, January 2008

[10] Bindeshwar Sing , Nupur Mittal , Dr. K.S. Verma, Dr. Deependra Singh , S.P. Singh , " Multi-level inverter: a literature survey on topologies and control strategies," *E-ISSN, Power Electron.*, vol. 10, pp. 2076-3336, July 2012.

[11] F. Forest, E. Labour´e, B. Gelis, V. Smet, T. Meynard, and J.-J. Huselstein, "Design of intercell transformers for high power multi-cell interleaved flyback converter," *IEEE Trans. Power Electron.*, vol. 24, no. 3, pp. 580– 591, Mar. 2009.

[12] D. A. Ruiz-Caballero and I. Barbi, "A new flyback-current-fed pushpull DC-DC converter," *IEEE Trans. Power Electron.*, vol. 14, no. 6, pp. 1056–1064, Nov. 1999.

[13] M. Gerber, J. A. Ferreira, I. W. Hofsajer, and N. Seliger, "High density packaging of the passive components in an automotive DC/DC converter," *IEEE Trans. Power Electron.*, vol. 20, no. 2, pp. 268–275, Mar. 2005.

[14] R.Watson, G. C. Hua, and F. C. Lee, "Characterization of an active clamp flyback for power factor correction applications," *IEEE Trans. Power Electron.*, vol. 11, no. 1, pp. 191–198, Jan. 1996.

[15] J. Biela, U. Badstuebner, and J. W. Kolar, "Impact of power density maximization on efficiency of DC–DC converter systems," *IEEE Trans. Power Electron.*, vol. 24, no. 1, pp. 288–300, Jan. 2009.